Study on SAR Distribution of Electromagnetic Exposure of 5G Mobile Antenna in Human Brain

Yaqiong Li[1] and Mai Lu[1,*]

[1] Key Laboratory of Opto-technology and Intelligent Control, Ministry of Education, Lanzhou Jiaotong University, Lanzhou 730070, China

[*] Corresponding author. E-mail: mai.lu@hotmail.com

Received: Oct. 20, 2019, Accepted: Jan. 13, 2020

Firstly, this paper establishes 5G mobile phone antenna and human head model. The performance characteristics of the two 5G mobile phone antennas were analyzed by HFSS (High Frequency Structure Simulator) software, and the electric field strength and specific absorption rate (SAR) distribution in the human head model under different antenna working frequency conditions were simulated. The simulation results show that: When the antenna operating frequency is 2600 MHz, the average SAR of any adjacent tissue with a mass of 10 g in the human head model is 0.217 W/kg, the peak of the electric field strength is 21.067 V/m, and the average frequency is 3500 MHz, the peak of the specific absorption rate is 0.285 W/kg, and the peak of the electric field strength is 22.844 V/m. Conclusion: Most of the electromagnetic field is absorbed by the scalp and skull near the antenna side. The SAR value reaching the brain is about 0.25 times of the total SAR value. The electric field strength is similar to the SAR value. As the distance between the brain region and the antenna increases, the SAR value decreases, and the SAR value in the brain is about 0.125 times that of the scalp. Compared with the limits set by the International Commission on Non-Ionizing Radiation Protection (ICNIRP), it is lower than the public electromagnetic exposure limit value 2 W/kg, which is in line with international standards.

Keywords: Mobile phone antenna; Electromagnetic exposure; Specific absorption rate; HFSS

http://dx.doi.org/10.6180/jase.202006_23(2).0012

1. Introduction

At present, the EU, the United States, South Korea, and Japan are actively promoting 5G development and deploying a series of strategic plans. At the same time, China also established the IMT-2020 (5G) promotion group in 2013. In 2016, the "13th Five-Year" National Informatization Planning and National Informatization Development Strategy listed 5G development as part of China's strategic planning. In November 2017, the Ministry of Industry and Information Technology officially announced the plan: 3300-3600MHz and 4800-5000MHz frequency band as the working frequency band of 5G system [1]. The Ministry of Industry and Information Technology said that it is expected that 5G mobile phone will be launched in the second half of 2019. According to the statistics of the Ministry of Industry and Information Technology, as of June 2019, the total number of mobile phone users in China reached 1.585 billion [2]. On May 31, 2011, the World Health Organization's International Agency for Research on Cancer (IARC) issued a statement stating that the use of mobile phones would increase the risk of cancer, and that cell phone radiation may have a causal relationship with cancer users' cancer [3]. Electromagnetic exposure for 2G/3G/4G(698–960 MHz, 1710–2690 MHz) mobile phones, many countries and organizations have conducted in-depth research. Reference [4] researched the phone at 900MHz, the influence of radiation power and gap distance on the SAR distribution of heads of different user's age. The results show that the mobile phone radiation SAR of the child's head is always higher than the adult head. Reference [5] studied the SAR of the human head under standardized conditions of two frequencies of 2G and 3G technologies of 897MHz and 1950MHz. Reference [6] studied the electromagnetic exposure of GSM mobile phones to human heads at 900MHz.

Internationally, the corresponding safety standards have been established for electromagnetic exposure of mobile phones. The International Non-Ionizing Radiation Protection Committee (ICNIRP) standard limit is 2W/kg [7]. China's Local Exposure Limits for Electromagnetic Radiation of Mobile Phones (GB21288-2007) is 2W/kg [8]. After 5G commercial, it will be a higher working frequency band and more users, so the electromagnetic exposure of the 5G mobile phone antenna to the human body cannot be ignored.

Therefore, based on the finite element method 3D electromagnetic simulation software HFSS (High Frequency Structure Simulator), two 5G mobile phone antennas are designed by coupling technology and parasitic patch technology, which are built-in Monopole folding antennas and Monopole planar antennas to realize 5G communication frequency band [9] coverage 3300-3600MHz, 4800-5000MHz. Firstly, the electromagnetic radiation characteristics of the antenna are simulated on the HFSS software. Then, the specific absorption rate value and electric field strength of the antenna at 2600MHz and 3500MHz of the 5G communication are calculated, and analyzes the spatial distribution, attenuation of SAR and electric field strength in human brain exposed to electromagnetic fields. Finally, the calculation results are compared with the public exposure limits in the Guidelines for Limiting Time-Varying Electric Fields, Magnetic Fields and Electromagnetic Exposures by the ICNIRP to analyze the safety of electromagnetic exposure of 5G mobile phone antennas to human bodies.

2. Establishment of finite element model

2.1. 5G mobile phone antenna structure

In this paper, the T-shaped and L-shaped Monopole antenna, which has been applied to 2G/3G/4G mobile phones, is improved, wide-banded, and two 5G mobile phone antennas are designed by using multi-branches, parasitic patches and coupling techniques [10].

The Monopole folded antenna structure is shown in Fig. 1(a). The antenna is printed on an FR4 dielectric substrate with a relative dielectric constant $\varepsilon_r = 4.4$ and a dielectric loss tangent $tan\delta = 0.02$.The size of the dielectric substrate is 120mm×60mm×0.8mm. The reference ground structure size is 105mm×60mm. The multi-band miniaturized Monopole folding antenna uses an asymmetric T-shaped monopole to couple the radiation patch. The upper side of the T-shaped monopole is a coupled rectangular radiation patch, and the width of the lower right corner of the patch leads to a width of the 0.5mm bent short-circuited branch serves to match the impedance and shorten the length of the resonant path, and can also generate a resonant mode at high frequencies. The upper left corner and the upper right corner of the rectangular patch respectively lead to a folded L-shaped branch with a height of 3.2mm, which serves to adjust the characteristic impedance of the antenna and increase the resonance mode, thereby realizing the broadband multi-frequency of the antenna. The radiating patch is coplanar with the reference ground. The feeding point of the antenna is located at the lower end of the T-shaped monopole and Feed with a 50-ohm microstrip line. The antenna excitation source is a lumped port excitation. Finally, band coverage of 0.765GHz-1.02GHz, 1.55GHz-3.85GHz, and 4.4GHz-4.5GHz is achieved.

The Monopole planar antenna structure is shown in Fig. 1(b). The antenna is printed on a 0.8 mm FR4 dielectric substrate with a relative dielectric constant $\varepsilon_r = 4.4$, a dielectric loss tangent $tan\delta = 0.02$, a substrate size of 75 mm × 140 mm × 0.8 mm, an antenna size of 41 mm × 8 mm, and a ground structure size of 75 mm × 132 mm, 30.5 mm × 5mm. The antenna consists of a planar L-shaped monopole antenna and an asymmetric S-shaped branch. At high frequencies, it acts as a resonance to excite multiple resonant modes. The ground plane consists of a double-branch structure and a rectangular structure. The double-branch structure acts as a coupling to a planar monopole antenna at low frequencies. The monopole antenna is printed on the top layer of the substrate and the ground plane is printed on the bottom layer. Feed with a 50-ohm microstrip line. The antenna excitation source is a lumped port excitation. The designed antennas have a return loss of less than -6dB and good pattern characteristics. The coverage band and size are suitable for current 5G smartphones. (Abbreviation: "Antenna1", "Antenna2")

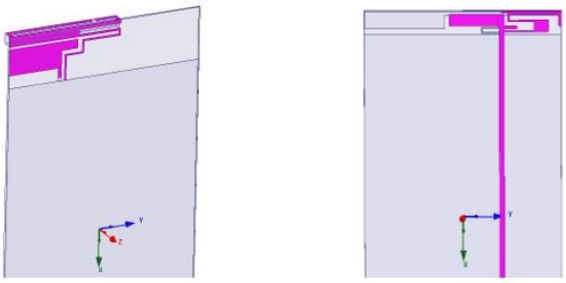

(a) Monopole folded antenna (b) Monopole planar antenna

Fig. 1. Antenna 3D models.

2.2. Human head model

Refer to the model proportion of the international common adult head. Establish a 3-layer head model [11]. The scalp radius is 0.092m, the skull radius is 0.085m, and the brain

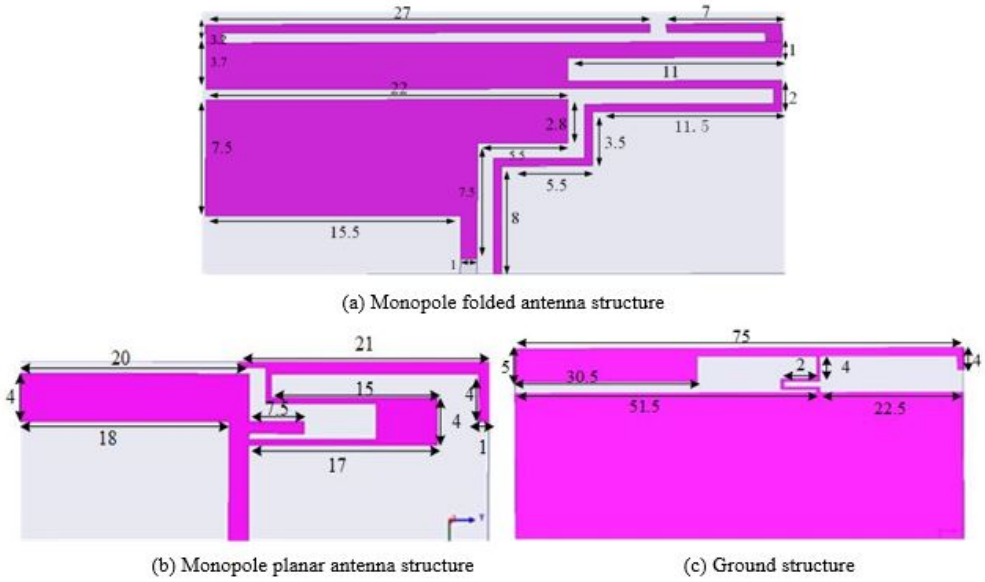

Fig. 2. Antenna structure size (unit: mm).

radius is 0.08 m. The 3-layer human head model is shown in Fig. 3.

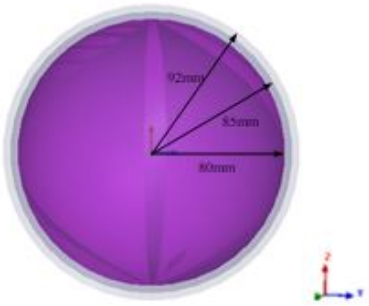

Fig. 3. Three-layer head model.

For the extraction of human tissue electrical parameters, the fourth-order Cole-Cole model [12] is generally used Administrator to calculate the electrical parameters of human tissue.

$$\varepsilon_r^* = \varepsilon_r^{'} - j\varepsilon_r^{''} = \varepsilon_{r\infty} + \sum_{n=0}^{4} \frac{\Delta\varepsilon_{rn}}{1+(j\omega\tau_n)^{1-\alpha}} + \frac{\sigma_i}{j\omega\varepsilon_0} \quad (1)$$

In the formula : ε_r^* is the complex relative dielectric constant; $\varepsilon_r^{'}$ is the relative dielectric constant (is the real part of ε_r^*); $\varepsilon_r^{''}$ is the loss factor (is the imaginary part of ε_r^*); $\varepsilon_{r\infty}$is the optical frequency relative dielectric constant value; $\Delta\varepsilon_{rn}$ is the relative dielectric constant increment; τ_n is the central relaxation time; α is the relaxation distribution time, the value is $0 \leq \alpha \leq 1$; ε_0 is the vacuum dielectric constant; σ_i is the ion conductivity; ω is the angular frequency.

Calculate the electrical parameters of the human head in different working frequencies by formula 1. The electrical parameters of the brain were averaged from the three tissues of cerebrospinal fluid, white matter and gray matter. The electrical parameters of the tissues of the head model are shown in Table 1. A method of taking the mean value of the dielectric constant to obtain a tissue parameter has been used in [13].

3. Simulation results and analysis

3.1. Antenna simulation results

3.1.1. Return loss S11

The simulation results of the S11 of the Monopole folded antenna are shown in Fig. 4. The results show that when S11<-6dB [14], the antenna can cover GSM850//900//1800//1900//UMTS//LTE2300//2500//Wi-MAX2300//2500//3500MHz band. The frequency band: 3300MHz—3800MHz and 4400MHz—4500MHz meet the 5G communication frequency band, providing more possibilities for 5G mobile communication. The simulation results of the S11 of the Monopole planar antenna are shown in Fig. 5. The results show that when S11<-6dB, the antenna can cover LTE700//GSM850//900//DCS//PCS//UMTS//LTE2300//2500//3500MHz//Wi-MAX3.5GHz//WLAN5.2GHz//5.8GHz band. Both high and low frequencies meet the design specifications and the 5G communication standard.

Table 1. Human head electrical parameters at different frequencies.

Tissue	Tissue density/(kg/m^3)	2600MHz		3500MHz	
		Relative permittivity	Conductance (S/m)	Relative permittivity	Conductance (S/m)
scalp	1100	42.645	1.684	41.473	2.308
skull	1850	11.293	0.424	10.793	0.614
brain	1030	42.330	1.603	41.154	2.223

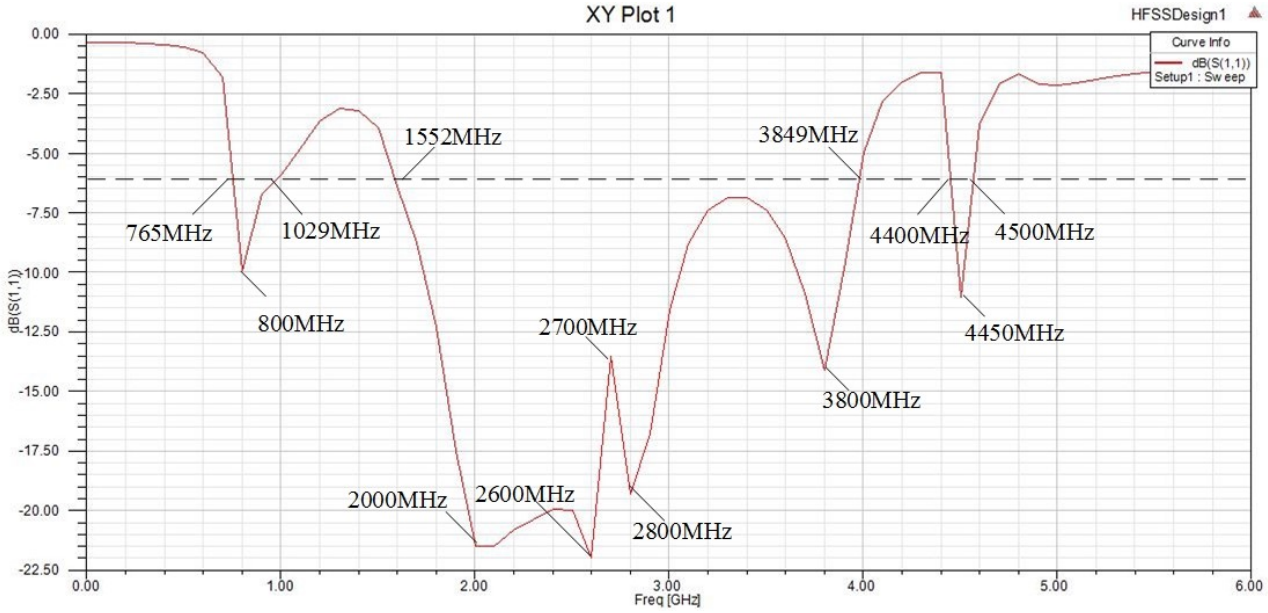

Fig. 4. Antenna1 S11 results of simulation.

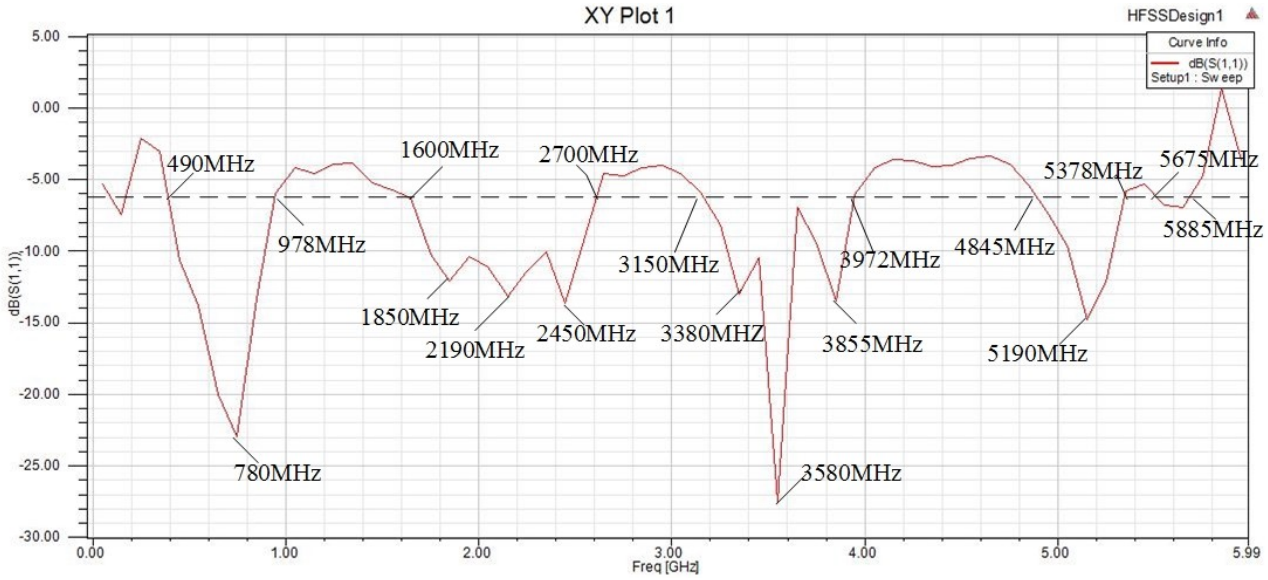

Fig. 5. Antenna2 S11 results of simulation.

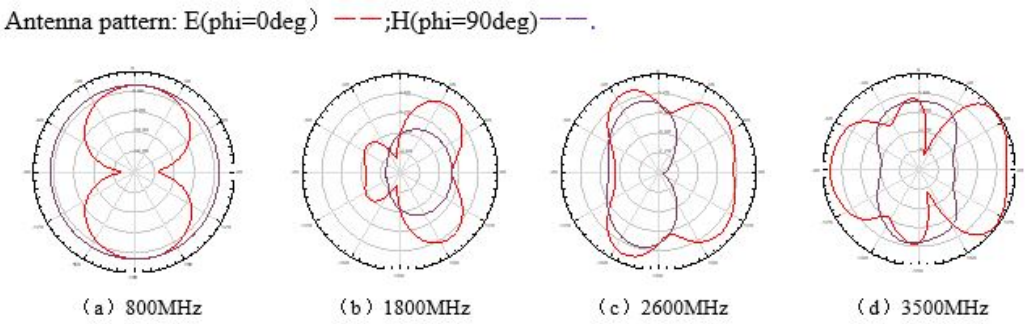

Fig. 6. Three-layer head model.

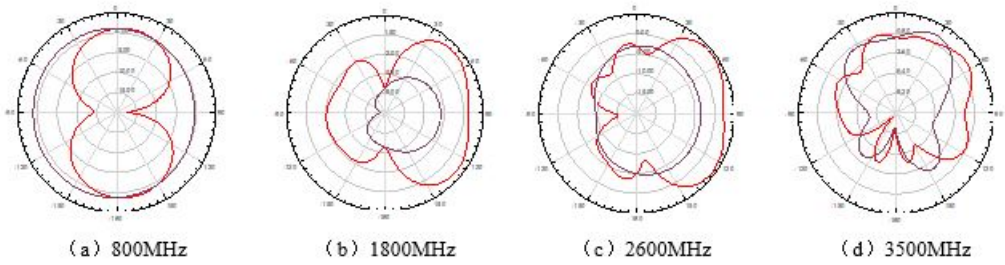

Fig. 7. Three-layer head model.

3.1.2. Antenna plane pattern

Fig. 6 and 7 show the E-H pattern characteristics of several important frequency points of the antenna in the whole frequency band. It can be seen from the figure that in the low frequency band of 800 MHz, the pattern has good radiation characteristics on the vertical plane, similar to the radiation characteristics of the half-wave dipole. As the frequency increases, the radiation characteristics of the antenna change. High-order mode excitation occurs in the high frequency bands of 1800MHz, 2600MHz and 3500MHz, so that the radiation intensity in one direction of the antenna increases, but the maximum radiation characteristics still exist in the vertical direction. Therefore, the gain of the maximum radiation direction of the high frequency band is increased compared to the low frequency part. Overall, the antenna radiation characteristics are better, meeting the requirements of mobile communications.

3.1.3. Current distribution

Fig. 8(a) is a surface current distribution diagram when the antenna operates at 800 MHz, and its current is mainly distributed on the coupling ground branch and the T-shaped monopole near the coupling branch. Fig. 8(b) shows the surface current distribution of the antenna operates at 1600MHz. The current on the coupled grounding branch is mainly distributed on the folded L-branch. It shows that the folding branch introduces a new resonance point, which affects the resonance characteristics of the antenna. The current distributions in Fig. 8(a) through 8(d) show that as the frequency increases, the effects of folding branches become more pronounced. The resonance of the antenna on the grounded coupling branch occurs mainly on the folded branches. The current zero present on the branches in the elliptical region in Fig. 8(c) divides the resonance of the entire antenna into two parts, namely the resonance of the side branches on the elliptical region and the resonance of the lower ground node and the monopole, both of which belong to strong resonances, which are close to each other and interfere with each other, affect the radiation characteristics of the antenna. The S11 parameter of the antenna in Fig. 4 produces a protrusion at 2700MHz, which also confirms this point. Fig. 9(a) is a surface current distribution diagram when the antenna works at 800MHz, and the current is mainly distributed on the coupled ground U-shaped branch and the L-shaped monopole. Fig. 9(c) shows the surface current distribution diagram of the antenna working at 2600MHz. The current on the coupled grounding branch is mainly distributed on the folded L-branch. It shows that the folded branch introduces a new resonance, which affects the resonant characteristics of the antenna. From the current distributions in Fig. 9(a) to 9(d), it is known that as the frequency increases, the influence of the S-shaped branch of the monopole antenna becomes

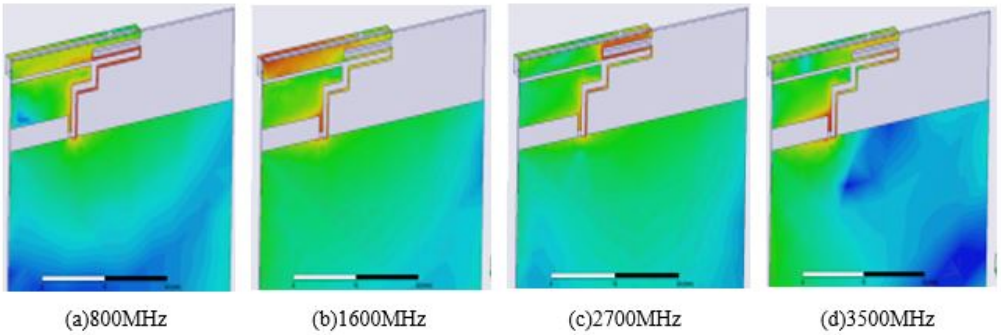

Fig. 8. Current distribution at different frequencies Antenna1.

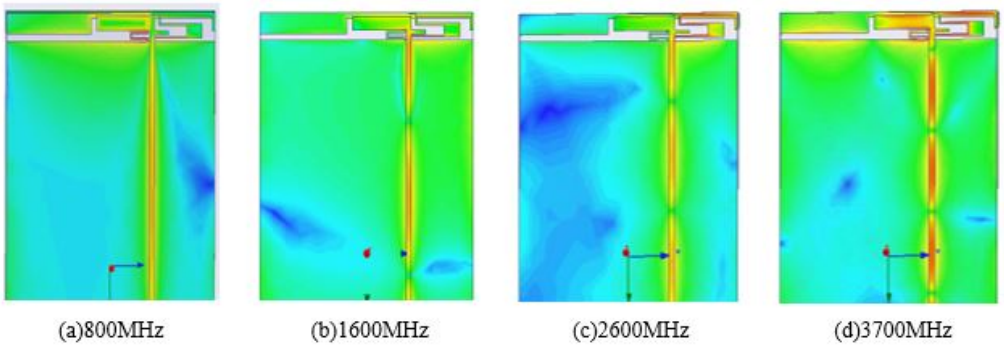

Fig. 9. Current distribution at different frequencies Antenna2.

more and more significant.

3.2. Distribution of electromagnetic dose in the head tissue

Calculate the distribution of SAR and electric field strength in the head model when the 5G mobile phone antenna is working at 2600MHz and 3500MHz, the antenna input power is 1W, and the head is 1.5 cm away, as shown in Fig. 10. Because the electromagnetic energy in biological tissues differs in the divergence and absorption of different tissue interfaces, the SAR value and electric field distribution of each tissue are not uniform. The results of electromagnetic dose in each tissue are shown in the table.

Table 2. Local SAR and average SAR Antenna1.

	SAR(W/kg)			
	2600MHz		3500MHz	
Tissue	SAR_{peak}	SAR_{10g}	SAR_{peak}	SAR_{10g}
scalp	3.237	0.991	5.399	1.760
skull	0.371	0.129	0.630	0.223
brain	0.975	0.305	1.299	0.341

From the SAR values in Table 2 and Table 3, when the mobile phone head is 1.5cm away and the frequency is 3500MHz. In the case of Antenna1, the average SAR of the scalp is 1.760W/kg, the skull is 0.223 W/kg and the brain is 0.341W/kg. In the case of Antenna2, the average SAR of the scalp is 1.629W/kg, the skull is 0.268W/kg, and the brain is 0.285W/kg. The scalp tissue absorbs more SAR than the brain and skull. The brain absorbs the least amount of SAR. This shows that the closer to the head when using the mobile phone, the greater the harm of the electromagnetic exposure of the mobile phone to the scalp. The average SAR in each of the above human head tissues is lower than the ICNIRP guideline with a limit of 2W/kg of 10g mass average, which meets safety standards. It can be seen from Table 4 and Table 5 that as the working frequency of the antenna increases, the electric field strength of each tissue increases. The electric field strength of the scalp

Table 3. Local SAR and average SAR Antenna2.

	SAR(W/kg)			
	2600MHz		3500MHz	
Tissue	SAR_{peak}	SAR_{10g}	SAR_{peak}	SAR_{10g}
scalp	1.292	0.595	4.870	1.629
skull	0.190	0.087	0.822	0.268
brain	0.755	0.217	0.908	0.285

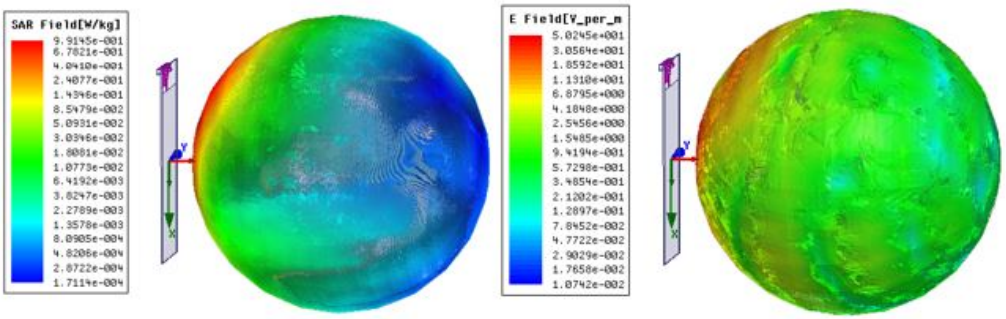

Fig. 10. 3D head tissue electromagnetic dose distribution.

Table 4. Local SAR and average SAR Antenna2.

Tissue	E(V/m)	
	2600MHz	3500MHz
scalp	50.245	57.399
skull	46.540	45.199
brain	26.064	26.857

Table 5. Electric field strength value Antenna2.

Tissue	E (V/m)	
	2600MHz	3500MHz
scalp	35.542	36.116
skull	35.257	31.787
brain	21.067	22.844

is greater than that of the brain and the skull, and the electric field strength of the brain is the smallest. It shows that as the distance from the antenna of the mobile phone to the head increases, the electric field strength gradually decreases. Compared with Antenna2, the ground clearance under Antenna1, when at the same frequency and the same distance, the average SAR and electric field strength of Antenna2 to the human brain are smaller than Antenna1. This shows that SAR may be significantly different as the antenna design changes.

Since the brain is one of the most important human tissues, it is composed of a large number of neurons, glial cells, vascular networks, and extracellular spaces. Therefore, the head model is taken as the starting point from the center cross section, and 1 slice is made every 15mm along the z-axis direction, the cut surface is made at 107 mm, 92 mm, 77 mm, 62 mm, 47 mm, 32 mm, and 17 mm. The distribution of the electromagnetic dose of each section is analyzed as shown in Fig. 11. Specifically, the SAR distribution and field strength distribution of the head tissues are analyzed when the two antennas work at 2600 MHz and

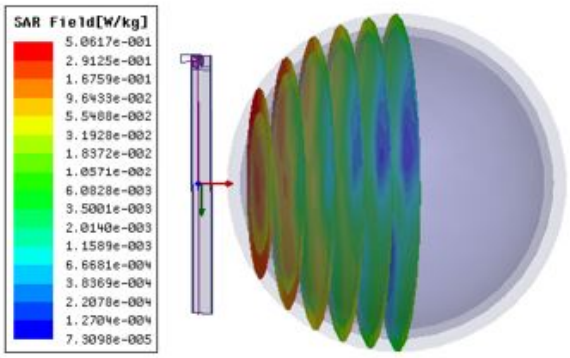

Fig. 11. Head SAR multi-section.

3500 MHz. Three sections at 107 mm, 77mm and 47 mm are selected to compare the SAR and electric field strength distribution.

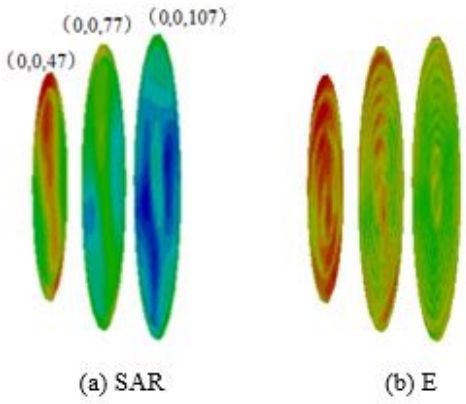

Fig. 12. Antenna1 Human head slice at 2600 MHz.

From Fig. 12(a) and 13(a), the closer the vertical distance to the antenna is, the more the average SAR is absorbed by the scalp and the brain. The average SAR of the head is mainly concentrated in the portion close to the antenna.

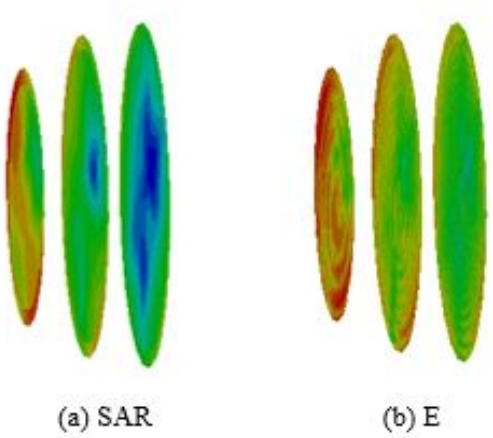

Fig. 13. Antenna1 Human head slice at 3500MHz.

It can be seen from Fig. 12(b) and 13(b) that the electric field strength decays very fast in the human head model, but there is still a certain amount of electric field energy penetrating into the brain. It shows that the external electric field can penetrate other tissues to reach the brain, which has a certain impact on the brain. The results show that: due to the different dielectric constants of the scalp, skull and brain, there are obvious mutations at the boundary of the three different tissues. The average SAR distribution in each tissue is quite different, and the average SAR of the scalp is obviously higher than other tissues. The electric field and SAR inside the brain are evenly distributed and are the smallest compared to other tissues. It can be seen

Table 6. SAR and E of different sections Antenna1.

	2600 MHz		3500 MHz	
Diameter section (mm)	SAR (W/kg)	E (V/m)	SAR (W/kg)	E (V/m)
(0, 0, 47)	$6.115x10^{-2}$	23.27	1.174	34.35
(0, 0, 77)	$5.525x10^{-2}$	9.30	$1.534x10^{-1}$	13.01
(0, 0, 107)	$1.630x10^{-2}$	3.77	$3.570x10^{-2}$	7.61

Table 7. SAR and E of different sections Antenna 2.

	2600 MHz		3500 MHz	
Diameter section (mm)	SAR (W/kg)	E (V/m)	SAR (W/kg)	E (V/m)
(0, 0, 47)	$3.242x10^{-1}$	26.04	1.487	32.25
(0, 0, 77)	$8.186x10^{-2}$	9.86	$3.049x10^{-2}$	14.72
(0, 0, 107)	$2.792x10^{-2}$	7.34	$6.780x10^{-2}$	9.18

from the above two tables that the maximum values of SAR and electric field strength are concentrated on the scalp tissue in the $(0, 0, 47)$ section. It shows that the closer the human tissue is to the antenna of the mobile phone, the more electromagnetic energy it absorbs.

Under the RF electromagnetic field exposure, the higher the working frequency, the closer to the antenna feed, the deeper the penetration depth of the average SAR and electric field strength in the brain.

Table 8. Comparison of SAR.

Reference	Frequency (MHz)	SAR (W/kg)
[15]	2600	0.425
[16]	2595	0.65
[17]	2700	0.48
[18]	3350	0.51
Proposed	2600	0.217
	3500	0.285

Compared with SAR values in literature [15], [16], [17], and [18] SAR values in this paper are the minimum at 2600MHz and 3500MHz, and far less than the electromagnetic exposure limit of ICNIRP of 2W/kg.

The comparison results in table 8 show that the study of SAR distribution of electromagnetic exposure of 5G mobile phone antenna in human brain in this paper is reliable and safe, which has reference value for the studying the high-frequency electromagnetic exposure of 5G mobile phone.

4. Conclusion

In this paper, through the modeling and numerical simulation of 5G mobile phone antenna, the SAR and electric field strength distribution of the human head under different working frequencies are compared. The calculation results show that when the input power of the two 5G mobile phone antennas is 1W, the distance from the human head is 1.5 cm, and the working frequency is 2600 MHz, the average SAR of the brain is 0.305 W/kg and 0.217 W/kg, respectively. When the working frequency is 3500 MHz, The average SAR of the brain is 0.341 W/kg and 0.285 W/kg, respectively, which accounted for 15% of the ICNIRP reference limit of 2 W/kg, which is much smaller than the public electromagnetic exposure limit established by ICNIRP. It shows that the 5G communication mobile phone antenna works in this high frequency electromagnetic environment is in compliance with safety standards, and will not pose a threat to health.

This paper only studies the safety of the antenna of the mobile phone to the human brain during parallel placement. After that, we need to study the distribution of SAR in the human brain when the antenna of the mobile phone

is tilted at different angles. With the development of mobile communication, the design of mobile phone structures and the emergence of new materials are worthy of attention for electromagnetic exposure of the human brain.

Acknowledgments

This research was financially supported by the National Natural Science Foundation of China (Grant Nos.51567015, 51867014), and by the Department of Education of Gansu Province under Grant 2018D-08.

References

[1] Ministry of Industry and Information Technology. Notice on the use of the 3300-3600MHz and 4800-5000MHz bands in the fifth generation mobile communication system. Technical report, Ministry of Industry and Information Technology, China, 2017.

[2] Ministry of Industry and Information Technology. Phone users in June 2019 by province. Technical report, Ministry of Industry and Information Technology, China, 2019.

[3] WHO. WHO 2011 Research Agenda for Radio Frequency Fields. Technical report, World Health Organization, 2011.

[4] Jafar Keshvari, Rahim Keshvari, and Sakari Lang. The effect of increase in dielectric values on specific absorption rate (SAR) in eye and head tissues following 900, 1800 and 2450 MHz radio frequency (RF) exposure. *Physics in Medicine & Biology*, 51(3):1463–1477, 2006.

[5] Simona Miclăuş, George Mihai, Angel Marian Aron, Cristian Mitrescu, Paul Bechet, and Octavian Baltag. Shielding Efficiency of a Fabric Based on Amorphous Glass-Covered Magnetic Microwires to Radiation Emitted by a Mobile Phone in 2G and 3G Communication Technologies. *Land Forces Academy Review*, 22(4):289–297, 2018.

[6] Deepshikha Bhargava, Nopbhorn Leeprechanon, Phadungsak Rattanadecho, and Teerapot Wessapan. Specific absorption rate and temperature elevation in the human head due to overexposure to mobile phone radiation with different usage patterns. *International Journal of Heat and Mass Transfer*, 130:1178–1188, 2019.

[7] G. Ziegelberger. ICNIRP statement on the "guidelines for limiting exposure to time-varying electric, magnetic, and electromagnetic fields (UP to 300 GHz)", 2009.

[8] GB21288-2007. Local exposure limit of electromagnetic radiation of mobile phones. Technical report, China, 2007.

[9] Yixin Li, Chow Yen Desmond Sim, Yong Luo, and Guangli Yang. 12-Port 5G Massive MIMO Antenna Array in Sub-6GHz Mobile Handset for LTE Bands 42/43/46 Applications. *IEEE Access*, 6:344–354, 2018.

[10] Qingwei Zhai, Jianfeng Li, and Lianghua Ye. Design of Planar Mobile Phone Antenna with small broadband and low ground effect. *Acta Electronica Sinica*, 39(8):1919–1922, 2011.

[11] S Rush and D. A. Driscoll. Current distribution in the brain from surface electrodes. *Anesthesia and Analgesia*, 47(6):717–723, 1968.

[12] S. Gabriel, R. W. Lau, and C. Gabriel. The dielectric properties of biological tissues: III. Parametric models for the dielectric spectrum of tissues. *Physics in Medicine and Biology*, 41(11):2271–2293, 1996.

[13] Wenying Zhou and Mai Lu. Health risk assessment of radio frequency electromagnetic field exposure of double-wood antenna in metro cabin. *High Voltage Engineering*, 42(8):2549–2557, 2016.

[14] Yong Ling Ban, Chuan Li, Chow Yen Desmond Sim, Gang Wu, and Kin Lu Wong. 4G/5G Multiple Antennas for Future Multi-Mode Smartphone Applications. *IEEE Access*, 4:2981–2988, 2016.

[15] Lakbir Belrhiti, Fatima Riouch, Abdelwahed Tribak, Jaouad Terhzaz, and Angel Mediavilla Sanchez. Calculating the SAR distribution in two human head models exposed to printed antenna with coupling feed for GSM/UMTS/LTE/WLAN operation in the mobile phone. *International Journal of Microwave and Optical Technology*, 11(6):391–398, 2016.

[16] Manoj Stanley, Yi Huang, Hanyang Wang, Hai Zhou, Zhihao Tian, and Qian Xu. A Novel Reconfigurable Metal Rim Integrated Open Slot Antenna for Octa-Band Smartphone Applications. *IEEE Transactions on Antennas and Propagation*, 65(7):3352–3363, 2017.

[17] Kuixi Yan, Peng Yang, Feng Yang, and Shao Ying Huang. Antenna design for a smartphone with a full metal casing and a narrow frame. *IET Microwaves, Antennas and Propagation*, 12(8):1316–1323, jul 2018.

[18] Z. M. Lwin and M. Yokota. Numerical analysis of SAR and temperature distribution in two dimensional human head model based on FDTD parameters and the polarization of electromagnetic wave. *AEU - International Journal of Electronics and Communications*, 104:91–98, 2019.